Environmental Science & Technology

Article

pubs.acs.org/est

First Dynamic Model of Dissolved Organic Carbon Derived Directly from High-Frequency Observations through Contiguous Storms

Timothy D. Jones, Nick A. Chappell,* and Wlodek Tych

Lancaster Environment Centre, Lancaster University, Lancaster LA1 4YQ, U.K.

Supporting Information

ABSTRACT: The first dynamic model of dissolved organic carbon (DOC) export in streams derived directly from high frequency (subhourly) observations sampled at a regular interval through contiguous storms is presented. The optimal model, identified using the recently developed RIVC algorithm, captured the rapid dynamics of DOC load from 15 min monitored rainfall with high simulation efficiencies and constrained uncertainty with a second-order (two-pathway) structure. Most of the DOC export in the four headwater basins studied was associated with the faster hydrometric pathway (also modeled in parallel), and was soon exhausted in the slower pathway. A delay in the DOC mobilization became apparent as the ambient temperatures increased. These features of the component pathways were quantified in the dynamic response characteristics (DRCs) identified by RIVC. The model and associated DRCs are intended as a foundation for a better understanding of storm-related DOC dynamics and predictability, given the increasing availability of subhourly DOC concentration data.

INTRODUCTION

Over the past three decades, surface waters in parts of North America and Europe have shown an increasing trend in dissolved organic carbon (DOC) concentration.[1] This has raised concerns within the water industry because of its impact on the formation of disinfection byproducts during raw water clarification.[2,3] As a consequence, some water utilities are now monitoring DOC concentrations within raw-water treatment works at a high frequency with automated spectrophotometers.[4] Furthermore, many of the factors (e.g., pH) that may be controlling the DOC trends[1] change rapidly over short periods, demanding high frequency observations to develop understanding of processes. In addition, some other processes may be sensitive to rapid changes in DOC concentration: notably, the acid−base chemistry of surface waters,[1,5] in-channel processing of nutrients such as nitrogen,[6] the release of organic micropollutants to streams,[7] and the bioavailability of metals in streams.[8] As a consequence, understanding subdaily dynamics in DOC concentration (DOC_{CONC}) and load (DOC_{LOAD}) in headwater streams is of concern to water resource engineers, aquatic ecologists, and water quality modelers.

Few regularly sampled records of DOC_{CONC} have been collected on a subdaily basis from either in situ monitoring or water sampling of natural streams and published. Where these data are available for headwater catchments dominated by mineral soils, DOC_{CONC} and DOC_{LOAD} change more through individual storm events rather than over seasonal time scales.[9,10] These storm-related changes occur over minutes to hours (e.g., Inamdar et al.[11]) and so demand subhourly monitoring to capture. This study addresses DOC dynamics within four microbasins (0.69−1.21 km^2) near to Llyn Brianne reservoir in upland Wales, UK.

When attempting to measure storm-related DOC_{LOAD} dynamics, under-sampling distorts the true DOC_{LOAD} signal

Received: July 19, 2014
Revised: October 17, 2014
Accepted: October 21, 2014
Published: October 21, 2014

through a phenomena known as temporal aliasing.[12] Any models based on under-sampled observations would have distorted (i.e., incorrect) parameter estimates, and the form of the model structure may be incorrectly defined or even unidentifiable when obtained directly from the observations. These effects are illustrated by Littlewood and Croke[13] for catchment models derived directly from rainfall and streamflow observations that are progressively under-sampled during numerical experiments. The need for a sufficient sampling rate to avoid these aliasing artifacts applies to both the development of data-based models and the validation of physics-based models. To avoid aliasing effects in hydrometric and water quality models, the minimum sampling rate should be determined from high-frequency data. These may be either existing observations or pilot data for the water quality variable of interest. Using these data, the minimum sampling rate can be estimated from the Nyquist rate (based on the Nyquist–Shannon sampling theorem[12]) or, preferably for noisy environmental observations, with the use of dynamic modeling.

Young[14] has demonstrated that one-sixth of the time constant (or TC/6) of a dynamic transfer function model[15] between rainfall and a catchment output variable (e.g., DOC_{LOAD}) is a robust measure of the minimum sampling rate required. For the study basins, Jones and Chappell[16] demonstrated that the minimum sampling rate (TC/6) required to capture dynamics in rainfall to hydrogen ion (H^+) load was 23 min. Given the possible association of DOC with H^+,[17,10] a 15 min sampling rate was chosen for observations of DOC_{CONC} and DOC_{LOAD} at these sites to avoid the effects of temporal aliasing. Given recent developments of field sensors for DOC measurement, notably field spectrophotometers covering the ultraviolet to visible (UV–vis) spectrum, such sampling rates can be maintained continuously. New stream monitoring studies using UV–vis sensors have mostly used the instrument known as a "spectrolyser" (scan Messtechnik GmbH, Vienna). These studies have used sampling rates of every 5 min,[18] 20 min[4] or 30 min[9,10,19,20] for periods ranging from 3.5 months[18] to 24 months.[9]

In recent years, there has been much concern over the use of catchment hydrochemistry models that produce highly uncertain results (and so, an inability to make realistic interpretations) by virtue of an overly complex model structure.[21] As a response to the need to constrain model uncertainty arising from structural complexity, there is considerable merit in following the principles of parsimony, that is, finding the simplest model able to simulate the observed dynamics in the variable(s) of interest. Dynamic models that are built directly from the information contained within time-series observations (i.e., data-based models without predetermined model structures) have the greatest potential to have parsimonious structures. Only a few dynamic models for the simulation of stream DOC_{CONC} (or DOC_{LOAD}) over time have been developed, notably the dynamic conceptual models of Hornberger et al.,[22] Taugbøl et al.,[23] Boyer et al.,[24,25] Futter et al.,[26,27] and Ågren et al.[28] These models differ from steady-state models of DOC (e.g., Grieve,[29] and Liu et al.[30]) in that dynamic models are able to simulate the effects of initial conditions or "memory effects" (i.e., effects of past values of DOC or associated mobilization processes or transport variables) as well as lags to response and exhaustion of stores. Although some of these dynamic models may be described as parsimonious, none have utilized regularly sampled, subdaily data from contiguous storm events or have had their structure (and associated parameters) derived directly from the dynamics contained within observed, subdaily time series of DOC_{LOAD} (i.e., data-based models).

This study has aimed to develop a dynamic, data-based model that is derived from and can explain most of the short-term changes observable within high quality DOC_{LOAD} observations (i.e., free from temporal aliasing, artifacts from sensor fouling, and calibrated to laboratory values) collected from a series of adjacent headwater streams. The specific objectives used to realize the aim were:

1. To develop the first dynamic model of stream DOC export derived directly from 15 min sampled observations continuously collected through contiguous rainstorms.
2. To develop understanding of the hydrological controls on rapid stream DOC dynamics through comparison of the models of four adjacent microbasins and with parallel analysis of rainfall to streamflow response.

■ EXPERIMENTAL SECTION

To explore the hydrological control on DOC_{LOAD} dynamics within streams of microcatchments draining upland soils (typical of humid temperate climates), four streams in close proximity were chosen for intensive monitoring (SI Figure S1). These streams drain into the Llyn Brianne water supply reservoir (52°8′7″ N 3°44′50″ W) on the upper reaches of the River Towy in the Cambrian Mountains, UK. Hydrological variables of rainfall and streamflow were measured using raingauges and flumes within the four basins (Supporting Information (SI) Figure S1); the characteristics of these basins are given in SI Table S1, with further details available in Jones and Chappell.[16]

A spectrolyser was installed at each of four streamwater quality stations (SI Figure S1). Details of the essential infrastructure designed for each spectrolyser are given in Supporting Information S1. Details of newly developed cleaning protocols required to minimize artifacts[31,32] within spectrolyser observations at Brianne are given in Supporting Information S2. All 256 spectral absorbance values monitored by each spectrolyser were data-logged every 15 min. Following transfer to a computer a proprietary algorithm ("RIVCOL": scan Messtechnik GmbH) was used to derive an initial estimate of DOC_{CONC} from a fixed set of these spectra. This initial estimate was then calibrated to absolute values of DOC_{CONC} for each time series of 16,141 values using 91 water samples collected between 11 Jan and 1 Oct 2013 from the Brianne streams covering low to high flows. These samples were analyzed (after filtering through 0.45 μm ash-less filter papers) by thermal oxidation and NDIR detector using a Shimadzu TOC-Vcph Analyzer (NPOC) at the Centralised Analytical Chemistry Group Laboratory of the Centre for Ecology and Hydrology (CEH). They ranged from 0.1 to 18 mg/L DOC_{CONC} and so covered the 0.33–10.28 mg/L range of calibrated DOC_{CONC} values derived from the spectrolyser spectra monitored at Brianne. The hydrometric and DOC observations selected for the exploratory modeling covered a 169 day period (8 Jan to 25 Jun 2013).

The essential first step in building data-based models (i.e., models in which the structure and parameters are derived directly from observations) is visualization of the observations to identify the basic class of model that may capture the

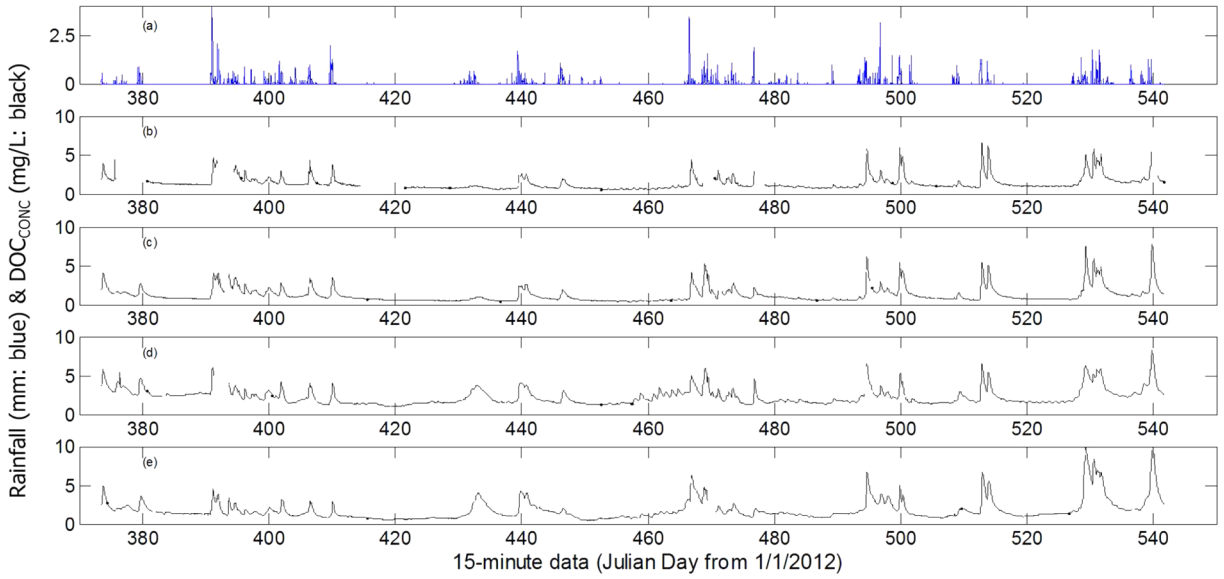

Figure 1. Time series of mean rainfall from the LI3 and LI6 raingauges (a), alongside DOC_{CONC} (at a 15 min monitoring rate) following quality assurance and local calibration of in situ UV−vis spectrophotometer measurements at water quality stations in grassland LI6 (b), grassland LI7 (c), forest LI3 (d), and forest LI8 (e), all near the Llyn Brianne reservoir. The first half of the data (Julian day from 1/1/2012 of 373.5208 to 460.9900) covers 8 Jan to 4 April 2013 (8398 values per stream), and the second half, 5 Apr to 25 Jun 2013 (day 461.0000 to 541.6458; 7743 values).

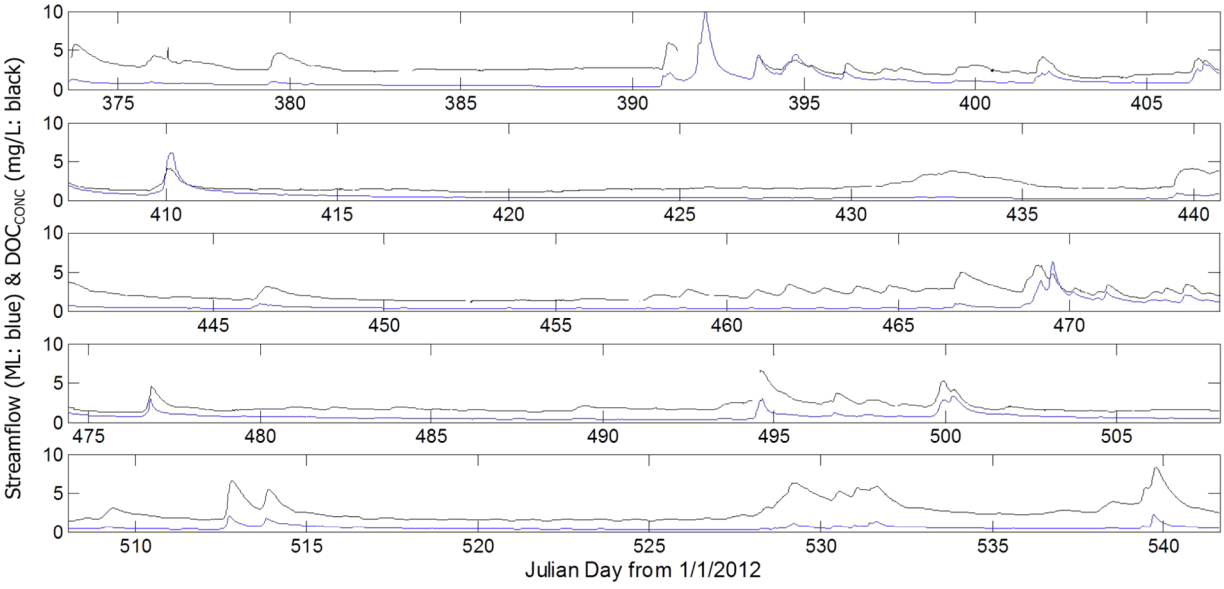

Figure 2. Full time series (8 Jan to 25 June 2013) of DOC concentration alongside streamflow (scaled/40) at LI3; similar time series for the other catchments are shown in SI Figures S2, S5, S8, and S11.

observed dynamic relationships.[33] Given that Jones and Chappell[16] identified a strong hydrological control on H^+ load for the same streams, the DOC_{CONC} and DOC_{LOAD} were first visualized with the rainfall and streamflow. Because the local relationship between rainfall and H^+ load involved inertia (i.e., dynamic delays and storage), it was considered likely that an algorithm capable of identifying data-based models that incorporate inertia would be needed. The RIVC algorithm (refined instrumental variable continuous-time Box−Jenkins identification algorithm) of Young[34] is one such procedure. Technically, RIVC implements an iterative instrumental variable (IV) method for estimation of general transfer functions that capture the dynamic relationship between input (e.g., rainfall) and output (e.g., DOC_{LOAD}) variables using rational polynomial expressions in operator s (in continuous time, e.g., eq 3), which directly translate to differential equations driven by the input variable (such as eq 2).[34] IVs are statistical tools, in this case current estimates of model output, that allow for unbiased estimation of the model parameters (e.g., α_1, α_2, β_0, β_1, and τ in eq 3). These IVs along with inputs and measured outputs are used within normal equations (originally introduced by Gauss) to obtain the parameter estimates and their covariance matrices. RIVC is part of the CAPTAIN Toolbox for MATLAB,[35] and greater explanation for the choice of RIVC to identify new models of DOC_{LOAD} and the associated parameters in the form of dynamic response characteristics (DRCs)[36] is given in Supporting Information S3.

Table 1. Optimal CT-TF Models of Rainfall-DOC_{LOAD} and Rainfall to Streamflow (Q) for both the 5th to 18th February 2013 Period and the 26th May to 5th June 2013 Period[a]

site	DOC_{LOAD}/Q	model[a]	YIC	R_t^2	TC_{fast} (h)	TC_{slow} (h)	fast %	slow %	SSG
LI3	Feb load	[2 2 3]	−5.60	0.904	4.96 ± 0.10	45 ± 12	56.5 ± 11	43.5 ± 11	1.595
	Feb Q	[2 2 2]	−6.65	0.904	4.99 ± 0.94	56 ± 58	24.5 ± 5.6	75.5 ± 5.6	0.703
	May load	[2 2 6]	−9.54	0.977	5.08 ± 0.03	87 ± 5.4	37.0 ± 2.4	62.0 ± 2.4	1.816
	May Q	[2 2 2]	−9.57	0.967	5.98 ± 0.01	175 ± 3.6	12.2 ± 2.2	87.8 ± 2.2	0.814
LI6	Feb load	[2 2 1]	−4.20	0.838	3.45 ± 0.11	32 ± 15	65.8 ± 15	34.2 ± 15	1.378
	Feb Q	[2 2 0]	−5.83	0.857	3.67 ± 0.65	50 ± 72	35.8 ± 5	64.2 ± 5	0.665
	May load	[2 2 9]	−8.50	0.953	2.29 ± 0.02	89 ± 2	44.0 ± 2.3	56.0 ± 2.3	1.557
	May Q	[2 2 5]	−9.92	0.961	2.72 ± 0.12	263 ± 270	10.9 ± 29	89.1 ± 29	1.050
LI7	Feb load	[2 2 1]	−3.76	0.838	4.76 ± 0.15	41 ± 29	68.8 ± 14	31.2 ± 14	1.170
	Feb Q	[2 2 0]	−5.82	0.857	4.73 ± 0.21	61 ± 43	31.5 ± 32	68.5 ± 32	0.630
	May load	[2 2 8]	−8.65	0.960	3.43 ± 0.02	44 ± 2	37.9 ± 24	62.1 ± 24	1.061
	May Q	[2 2 0]	−9.32	0.956	11.03 ± 0.48	373 ± 290	12.0 ± 31	88.0 ± 31	1.120
LI8	Feb load	[2 2 2]	−5.27	0.870	5.09 ± 0.14	46 ± 21	47.4 ± 14	52.6 ± 14	2.155
	Feb Q	[2 2 2]	−6.35	0.883	3.48 ± 0.16	63 ± 120	16.3 ± 32	83.7 ± 32	1.407
	May load	[2 2 8]	−8.52	0.972	10.98 ± 0.13	372 ± 94	34.9 ± 6.6	65.1 ± 6.6	4.315
	May Q	[2 2 1]	−9.46	0.949	7.77 ± 0.35	441 ± 120	6.5 ± 27	93.5 ± 27	2.589

[a]Model structure[a] is given as [denominators, numerators, pure time delays], and parameter estimates are given in SI Table S10. All TC (in hours) and pathway percentages are shown with uncertainty from 1000 Monte Carlo realizations.

Several studies have indicated that seasonal changes in air temperature may affect DOC production within soil water.[37,38] As a result, the study separately applied the RIVC routine to contiguous storms over the 5 to 18 Feb period and to contiguous storms over the 26 May to 5 June period that had different temperatures as well as different hydrometric characteristics. Applying the model identification to two separate periods also allowed conditional validation[39] of the model structures identified.

RESULTS AND DISCUSSION

Local DOC Calibration of the RIVCOL Algorithm for the Brianne Streams. Ninety-one water samples were analyzed in the laboratory to derive a local calibration of the spectrolyser data. This calibration relates an initial estimate of concentration derived from "cleaned spectra" (see Supporting Information S2) using the proprietary RIVCOL algorithm (DOC_{RIVCOL}) to absolute values of DOC_{CONC} (mg/L) measured in the laboratory and is shown in eq 1:

$$DOC_{CONC} = (DOC_{RIVCOL} \times 0.5374) + 0.0045 \quad R^2 = 0.99 \tag{1}$$

For the Brianne streams, RIVCOL therefore overestimated the DOC_{CONC} by a factor of 1.8−1.9 and demonstrates the importance of local calibration. Calibrating in the same way, Joeng et al.[18] found that RIVCOL produced stream DOC estimates for the Haean Basin (South Korea) that were a factor of 0.3 (for low true DOC values) to 1.3 (high true DOC values) those determined in the laboratory. In contrast, Jollymore et al.[9] found that RIVCOL produced DOC estimates for streams in a headwater catchment in British Columbia (Canada) that were a factor of 0.95 (high true DOC values) to 1.8 (low true DOC values) of those determined in the laboratory. The resultant quality assured and calibrated DOC_{CONC} for the 8 Jan to 25 June period is shown in Figure 1. These 15 min sampled data cover the end of a relatively cold period between 8 Jan to 4 Apr with mean stream temperatures at LI6 of 3.4 °C and a subsequent period 5 Apr to 25 June at 8.71 °C.

Visualization of DOC_{CONC}, DOC_{LOAD}, Rainfall and Streamflow. Marked peaks in DOC_{CONC} are associated with the streamflow hydrographs that follow the peaks in rainfall (Figure 1 and Figure 2). This storm-related change in DOC_{CONC} often occurs over short periods of less than 1 day (Figure 2). This underlines the importance of a subdaily monitoring regime for DOC_{CONC}. The rate of increase in DOC_{CONC} in response to a rain storm is typically comparable to those of the streamflow response, although the recession of DOC_{CONC} is sometimes slower than the streamflow recession (Figure 2).

Over the 169 day winter-to-spring period, the range of the locally calibrated DOC_{CONC} data for the LI6 stream was 0.52−6.53 mg/L, whereas at LI7, it was 0.33−7.80 mg/L; LI3, 1.04−8.28 mg/L; and LI8, 0.47−10.28 mg/L, respectively (Figure 1). The similar ranges in DOC may be expected from the similar proportions of each basin covered by peat and peaty-gley soils (FAO-UNESCO Histosol and Humid Gleysol) versus podzolic soils (SI Table S1 and SI Figure S1). The slightly higher maxima for storms within the forested basins (Figure 1de) may be related to the greater release of DOC from drained conifer plantation soils relative to adjacent grassland soils.[40] The very large streamflow peak during day 392 (Figure 2) is associated with a rare snowmelt event, but this period was not explored further because of a 3 day gap in the DOC record at this time.

Plotting 15 min sampled DOC_{CONC} against streamflow produced distinct hysteresis loops for each storm (SI Figures S14−S17). Although each loop shows increasing DOC_{CONC} with increasing streamflow, as observed by Hinton et al.,[41] Dawson et al.,[42] and Strohmeier et al.,[10] differences in the DOC_{CONC} to streamflow relation between the rising and falling stage of each hydrograph produces a pronounced loop that has a different shape between different storms. This demonstrates that DOC_{CONC} responses are out of phase with the streamflow, necessitating the use of dynamic data-based models to capture the effects of storage. A similar complexity was observed in the relationship between rainfall and streamflow, likewise indicating that the rainfall−streamflow relation sampled at a high frequency is not a purely instantaneous response, but one involving a dynamic internal state. Given that dissolved solutes,

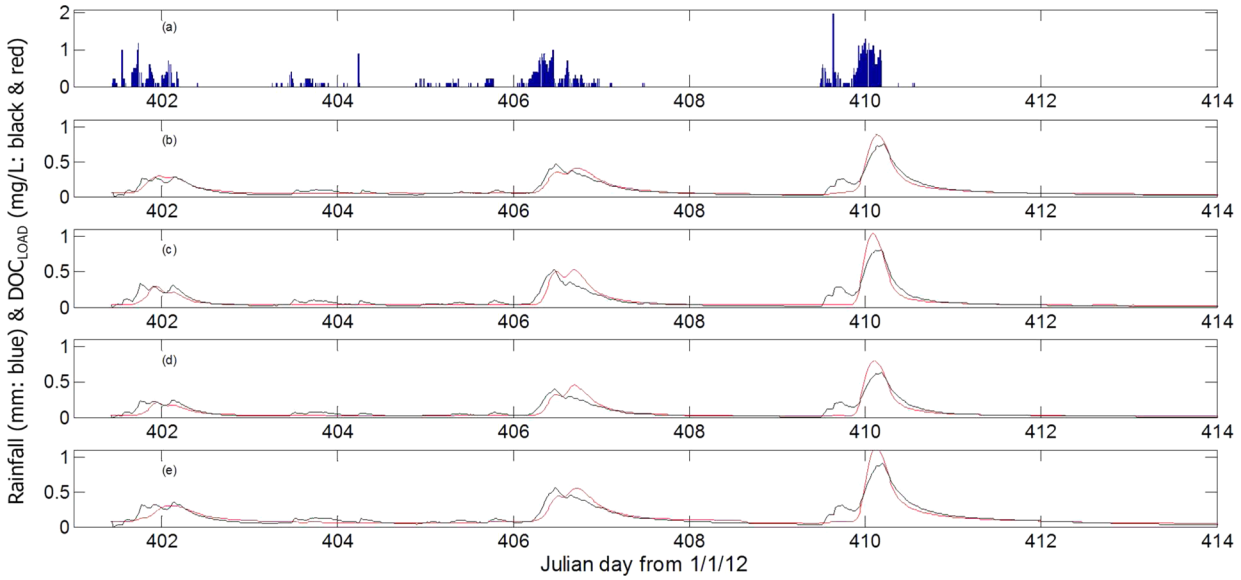

Figure 3. Rainfall (a) and simulated DOC load (black line) and observed DOC load (red line) for optimal second-order CT-TF models of (b) LI3 stream, (c) LI6 stream, (d) LI7 stream, and (e) LI8 stream for the contiguous storms over the 5−18 February 2013 period. Comparable results for the period 26 May to 5 June 2013 are shown in SI Figure S19.

such as DOC, move along the subsurface (and surface) hydrological pathways associated with the rainfall−streamflow response,[43,44] it would not be surprising if the relation between rainfall and stream DOC_{CONC} or DOC_{LOAD} also exhibits short-term storage effects (rather than a solely instantaneous response) and thereby require dynamic data-based modeling.

Comparison of DOC_{CONC} with DOC_{LOAD} time series (SI Figures S3, S6, S9, and S12) shows that the DOC export is often more flashy or rapidly exhausted when compared with concentration within the stream (e.g., the simple event on day 410 in SI Figure S3). Consequently, analysis of DOC export requires a greater monitoring frequency than even the rapid dynamics in the concentration would suggest. Examination of the timing of the export of DOC mass (kg/15 min) relative to the export of the water mass or volume, that is, ML/15 min (SI Figures S4, S7, S10 and S13), perhaps allows the most robust visual interpretation, given that both are fluxes (a concentration is a "state" not a "flux", and so comparison with waterflow is more difficult to interpret directly). The initial recessions in the load and streamflow time series seem broadly comparable, but the later recessions are slower for the streamflow in comparison with the DOC_{LOAD} (e.g., SI Figure S4). Given that streamflow recessions of several hours to a few days are often associated with drainage from the subsoil or underlying regolith,[16] the more rapid later recession in DOC_{LOAD} may indicate that much less DOC mass is transported by these deeper pathways and is soon exhausted. Relative to the streamflow, the peaks in DOC_{LOAD} within storm periods are larger within the warmer spring period (e.g., days 510 to 540) compared with the cooler winter period (e.g., days 395 to 425; e.g., SI Figure S4).

Identified Dynamic Models of DOC_{LOAD} in Relation to Hydrological Response. A key objective of the data-based modeling was to identify features observed in the data visualization within model parameters and DRCs. Given that the peaks in DOC_{LOAD} and DOC_{CONC} seem to be associated with those in streamflow (e.g., Figure 2), models capable of simulating streamflow response may have structures and input variables (e.g., rainfall) suitable for simulating the dominant mode of behavior of stream DOC_{LOAD} when observed at the same high frequency.

Table 1 shows that application of the RIVC algorithm to the 15 min DOC_{LOAD} and streamflow data (output variables) from the 15 min rainfall data (input variable) produced optimal continuous-time transfer function (CT-TF) models with high simulation efficiencies. Within this model development study, the procedures for identifying the optimal model structure using statistical measures of simulation efficiency and parsimony[45,46] are given in SI S4. The model structures with the highest 20 simulation efficiencies when the algorithm was applied to the DOC_{LOAD} values are shown in SI Tables S2−S9.

Table 1, Figure 3, and SI Figure S19 show that the optimal dynamic models of stream DOC_{LOAD} given an input of rainfall are able to explain 84−97% of the observed dynamics through contiguous storms. This demonstrates that when the components of DOC_{LOAD} (i.e., streamflow and DOC_{CONC}) are adequately sampled (here continuously monitored in situ every 15 min), most of its dynamics through a sequence of storms can be simulated from hydrometric (i.e., rainfall) data alone.

The RIVC algorithm, combined with model selection criteria, indicates that the rainfall to stream DOC_{LOAD} dynamics are best characterized by a second-order [2 2 τ] CT-TF model structure (Table 1). The form of this model can be expressed in ordinary differential equation terms (ignoring initial conditions):

$$\frac{d^2L_{DOC}(t)}{dt^2} + \alpha_1\frac{dL_{DOC}(t)}{dt} + \alpha_2 L_{DOC}(t) = \beta_0\frac{dr(t-\tau)}{dt} + \beta_1 r(t-\tau) \quad (2)$$

where L_{DOC} is the stream DOC_{LOAD} (kg/15 min), r is the rainfall average from the LI3 and LI6 raingauges (mm/15 min), τ is the pure time delay between rainfall and an initial DOC_{LOAD} response (number of 15 min periods), α_1 and α_2 are the parameters capturing the rate of DOC exhaustion (/15 min), β_0 and β_1 the parameters capturing the magnitude of DOC production or gain (kg 15 min/mm), and t is time in 15

min periods. The same model can be expressed as a second-order transfer function in continuous-time (CT-TF):

$$L_{DOC} = \left(\frac{\beta_0 s + \beta_1}{s^2 + \alpha_1 s + \alpha_2}\right) e^{-s\tau} r; \quad S \sim \frac{d}{dt} \tag{3}$$

where s is the Laplace operator. To permit physical interpretation, this second-order transfer function model of DOC_{LOAD} can be decomposed by partial fraction expansion[15] (using the "Residue" function in Matlab) into two parallel, first-order transfer functions:

$$L_{DOC} = \frac{\beta_f}{s - \alpha_f} e^{-s\tau} r + \frac{\beta_s}{s - \alpha_s} e^{-s\tau} r \tag{4}$$

where α_f and α_s are the parameters capturing the rate of DOC exhaustion of the fast and slow components that comprise the total DOC load, respectively (/15 min), and β_f and β_s are the parameters capturing the magnitude of DOC production or gain of the fast and slow components, respectively (kg 15 min/mm). As an illustration, eq 5 shows values of parameters given in eq 4 for the model of stream DOC_{LOAD} for the LI3 basin during the selected February period (and with three pure time delays, i.e., a [2 2 3] model):

$$L_{DOC} = \underset{\text{Fast}}{\frac{0.0454}{s + 0.0504}} e^{-3\Delta t s} r + \underset{\text{Slow}}{\frac{0.00379}{s + 0.00546}} e^{-3\Delta t s} r \tag{5}$$

where Δt is the time-step in the observations (here, 15 min). These values and those from all models are shown in SI Table S10. The observation that all four streams and both periods modeled independently exhibit the same purely linear, second-order model structure (Table 1) provides some conditional validation[39] of the DOC model robustness at this locality.

Interpretation of the High-Frequency DOC_{LOAD} Dynamics Observed with the Aid of Modeling and Comparison with Hydrometric Dynamics. A purely linear, second-order CT-TF model that can be decomposed into two parallel, first-order CT-TFs suggests that the stream DOC_{LOAD} response through a period of contiguous storms comprises two parallel catchment stores that deliver DOC mass to streams with differing rates of production (gain) and exhaustion (recession) after a rainfall stimulus. For the same basins and periods, RIVC indicates that the rainfall to streamflow response is similarly characterized by a second-order model structure (Table 1). This might suggest that the stream DOC_{LOAD} dynamics result from the same two water pathways responsible for the streamflow response. Consequently, comparison of the delivery behavior of these two stores for DOC mass with that of the hydrometric response may reveal additional DOC-related characteristics of these stores.

Physical interpretation of the behavior of the model stores is always made after first calculating the DRCs[16,36] of component transfer functions from parameters α_f, α_s, β_f, β_s and τ given in eq 4. These DRCs include the time constant (TC) for each component, store, or pathway, which for the fast path is given as

$$TC_{fast} = \frac{\Delta t}{\alpha_f} \tag{6}$$

A further DRC is the steady-state gain (SSG) of all components combined and when defined for a second-order CT-TF model is the quotient of the β_1 and α_2 parameters because the other parameters (α_1 and β_0 in eq 3) involve derivatives or s-operators and so are zero at steady-state.

$$SSG = \frac{\beta_1}{\alpha_2} \tag{7}$$

For the DOC_{LOAD} models presented, the steady-state gain (kg/mm) is the time-integrated DOC mass simulated from the observed time-integrated rainfall and can be used to calculate the proportion of the DOC mass response from each store. For example, the proportion of the DOC mass response from the most rapidly draining of two parallel stores (Fast %) is given as

$$\text{Fast\%} = 100\left(\frac{SSG_1}{SSG_1 + SSG_2}\right) \tag{8}$$

where SSG_1 and SSG_2 are the steady state gains of the fast and slow first-order stores (for a CT-TF model), respectively. Given the linearity of the DOC system through periods of contiguous storms, the time constant is a measure of how quickly (in periods of the data time-step or converted to hours) each DOC store is exhausted to 37% of the peak in DOC mass exported. The DRCs of the rainfall-streamflow system can be interpreted in the same way as the rainfall-DOC system, but for the components of the hydrometric response. For example, SSG is the simulated runoff coefficient if streamflow is presented as a discharge per unit basin area.

In comparison with the hydrometric response, considerably more DOC_{LOAD} is exported by the fast response component (Fast %: eq 8) by a factor of 1.8−5.4 within both periods modeled (Table 1). Given that the fast hydrometric response is often associated with shallow water pathways, including those interpreted at the study sites[16] and measured directly elsewhere in the Cambrian Mountains,[47] this result (uniquely obtained directly from the dynamics in the observations) would suggest that shallow water pathways have much greater releases of DOC than deeper water pathways. This finding is consistent with the observation that DOC_{CONC} within mobile pore waters at Brianne is greater in the near-surface strata of the podzolic soils compared with deeper strata.[48] In addition, many conceptual models of DOC transport to streams (e.g., Boyer et al.,[25] Futter et al.[26]) need to route a significant proportion of DOC via a shallow water path to simulate stream DOC_{CONC} consistent with observations. Examining the time constants shows that the rate of exhaustion of the fast component of the DOC_{LOAD} (eq 6) is for the most part comparable to the rate of drainage of the fast water flow. In some contrast, the rate of exhaustion of the delayed component of the DOC_{LOAD} (TC_{slow} in Table 1) is much faster than the rate of drainage of the delayed water-flow component by a factor of 1.4−2.2. These model-derived findings are consistent with the earlier data visualization and with the smaller contribution from the delayed DOC pathway (Slow % in Table 1). An "exhaustion effect" following a storm peak in stream DOC_{CONC} or DOC_{LOAD} has been observed by Worrall et al.,[49] Hood et al.,[50] and Morel et al.[51] and in H^+ load within the same Brianne streams.[16] The exhaustion effect at Brianne may imply the rate of DOC release into mobile water within the near-surface strata is limited so that continued drainage of mobile water into the subsoil (and thence, to the stream via the deeper pathway) becomes progressively diluted in DOC_{CONC} following a storm peak.

During the May simulation period, the proportion of DOC mass delivered by the fast component reduced by a factor of 0.55−0.74 in the four streams compared with the February

period (Table 1). This is consistent with the smaller proportion of the hydrometric response from fast, shallow pathways at all sites during the drier May period (Figure 1) and, hence, reduced DOC flushing from shallow pathways. A shift in the timing of the DOC delivery between the February and May periods is clear within the pure time delay between a rainfall stimulus and initial response in the simulated DOC_{LOAD} (Table 1). The pure time delay between the February and May periods systematically increases for all four basins by up to 120 min (e.g., from a [2 2 1] to [2 2 9] model of the LI6 DOC export), whereas streamflow does not show a consistent shift between the two periods. The initial wetting of very dry organic surface strata can result in "new water" bypassing the matrix in macropores, thereby delivering water to streams having had little interaction with the solute-rich matrix waters.[52] This would delay the first arrival of DOC-rich waters in the streams. Equally, lateral flow generated in saturated wedges at the base of near-surface organic strata of podzolic soils, as noted by Chappell et al.[47] elsewhere in the Cambrian Mountains, will take longer to develop during drier antecedent conditions. This could lead to a delay in the first delivery of DOC-rich water from O horizons of podzols relative to water displaced from deeper strata (e.g., B/C or C horizons) containing less DOC.[43,47] The increase in SSG of the whole DOC_{LOAD} response between the January and May periods by an average factor of 1.34 may be explained by the increase in the SSG of the rainfall-streamflow system by a factor of 1.59 (Table 1).

The TCs for the fast components of the DOC_{LOAD} response ranged from 2.29 ± 0.02 to 10.98 ± 0.13 h, whereas those for the fast hydrometric response ranged from 2.72 ± 0.12 to 11.03 ± 5.37 h (Table 1). To adequately sample the recessions that the TC_{fast} values characterize requires the observation of at least six evenly spaced temporal samples within the period of the TC_{fast}.[14] Thus, for the fastest responses observed across these four headwater basins, the streamflow (and associated rainfall) must be recorded at least every 0.45 h or 27 min (i.e., 2.72/6 h), and DOC_{LOAD} (and associated rainfall, DOC_{CONC} and streamflow) must be recorded at least every 0.38 h or 23 min (i.e., 2.29/6 h). The effect on TC_{fast} of sampling DOC_{LOAD} less frequently than the minimum 23 min is shown in SI Figure S20 for LI3 data in the February period. All interpretations presented within this study were based on variables recorded every 15 min and so avoided any aliasing effect on TC_{fast}. Observational data sets associated with previous DOC modeling studies[22−28] do not have this sustained intensity of DOC monitoring. As a result, these studies may not have observations sufficient to prevent temporal aliasing in the DOC_{LOAD} dynamics and resultant model parameters. Consequently, the data sets used in these previous studies may be insufficiently detailed to allow conditional validation of the dynamics simulated or model parameters estimated. Prevention of temporal aliasing needs to be a core priority within all future DOC modeling studies.

In summary, this study is the first to derive a dynamic model of stream DOC_{LOAD} directly from regular subdaily observations through contiguous storm events. The information contained within the 15 min observations indicates that the rainfall-to-DOC export system in the selected upland headwaters consisted of two dominant components, each with purely linear dynamics. Given that independent application of the RIVC algorithm to the four nearby basins and two separate periods produce the same optimal model structure, this structure would seem to be relatively robust at this locality. This is further reinforced with the finding that the optimal model structure is identical to that of the rainfall-to-streamflow model (and rainfall-to-H^+ load[16]) determined independently. This contrasts with previous approaches to modeling stream DOC that have forced DOC transport to follow one, two, or more pathways fixed prior to the modeling. The similarity of the model structures, combined with high simulation efficiencies and relatively low parametric uncertainties, has permitted preliminary physical interpretation of dynamic response characteristics identified by the RIVC algorithm.

Through periods of contiguous storms, the high frequency dynamics in rainfall are as important to simulating DOC_{LOAD} within streams as they are to simulating streamflow itself, demonstrating the strong hydrological control on the export of DOC from headwaters. With reference to the parallel hydrometric modeling, several findings could be extracted from the observed dynamics in DOC_{LOAD}. First, most of the DOC export was associated with the faster hydrometric pathway, and that within the slower pathway is soon exhausted. Second, as ambient temperatures increase between winter and spring, the delay between a rainfall input and DOC mobilization increases significantly, potentially indicating a disconnect between the initial hydrometric response and DOC transport. Third, exploration of the dynamics in the DOC_{LOAD} using RIVC has demonstrated that the 15 min monitoring utilized in these headwaters met the Young[14] criterion to avoid temporal aliasing of the fundamental, storm-related dynamics. This implies that future studies that aim to collect DOC_{CONC} and DOC_{LOAD} observations in headwater streams for subsequent modeling may need to consider the use of similarly high monitoring intensities.

The simulated dynamics identified by the approach utilizing the RIVC algorithm that include estimates of delays to initial response, relative importance of different DOC sources and hydrological pathways, and rates of exhaustion of mobile DOC stores are considered preliminary interpretations. This is to encourage others to obtain independent observations of the dynamics of potential component pathways (e.g., lateral flow within an O-horizon[47]) to support or reject the components identified from the whole-basin response.[16] The approach also indicates the potential for extending single simulations across seasons by including other variables, such as temperature[53,54] or measures of microbial activity in addition to rainfall within multiple-input, single-output (MISO) models of DOC export. Adding additional variables may allow the model to explain more of the dynamics in DOC_{LOAD} than possible with the model presented in eq 3. Furthermore, in situ UV−vis spectrophotometers such as the "spectrolyser" record a wide range of absorbance values for which certain wavelengths may be associated with the properties of the carbon being transported in streams.[55] MISO modeling of the specific spectral wavelengths combined with stream or climatic variables may allow deeper understanding of the dynamics of DOC export during storms and directly address the needs of the water industry[56] in regions with a rising DOC trend.

■ ASSOCIATED CONTENT

Supporting Information

Exact details of the essential infrastructure designed for each spectrolyser (section S1); findings of the cleaning protocols developed to deliver high quality DOC time-series (section S2); rationale for use of the RIVC algorithm for model identification (section S3); the procedure for identifying the

optimal model structure using statistical measures of simulation efficiency and parsimony (section S4); details of the study basins (Table S1); most efficient 20 rainfall-DOC_{LOAD} models for all basins (Tables S2−9); parameters identified for optimum models (Table S10); location of monitoring equipment and organic-rich soils (Figure S1); DOC_{CONC} and DOC_{LOAD} together with streamflow for all basins (Figures S2−S17); DOC_{LOAD} observations and simulations plus rainfall (Figures S18−S19); and an example of the effect on TC_{fast} of undersampling DOC_{LOAD} (Figure S20). This material is available free of charge via the Internet at http://pubs.acs.org

AUTHOR INFORMATION

Corresponding Author

*Phone: +44 1524593933; fax: +44 1524843087; e-mail: n.chappell@lancaster.ac.uk.

Funding

Funding was provided by Natural Environment Research Council Grant NE/J014826/1 (DURESS-Lancaster project within the NERC Biodiversity & Ecosystem Service Sustainability program).

Notes

The authors declare no competing financial interest.

ACKNOWLEDGMENTS

The authors thank the landowners for access to the research basins. Dr. Gloria Dos Santos Pereira (Head of the Centralised Analytical Chemistry Group Laboratory of the Centre for Ecology and Hydrology) and Mr. Joe Compton are thanked for their help with the sampling and analysis of the DOC calibration data.

REFERENCES

(1) Evans, C. D.; Jones, T. G.; Burden, A.; Ostle, N.; Zieliński, P.; Cooper, M. D. A.; Peacock, M.; Clark, J. M.; Oulehle, F.; Cooper, D.; Freeman, C. Acidity controls on dissolved organic carbon mobility in organic soils. *Global Change Biol.* **2012**, *18*, 3317−3331.

(2) Kay, P.; Edwards, A. C.; Foulger, M. A review of the efficacy of contemporary agricultural stewardship measures for ameliorating water pollution problems of key concern to the UK water industry. *Agric. Syst.* **2009**, *99*, 67−75.

(3) Chow, A. T.; Dahlgreen, R. A.; Zhang, Q.; Wong, P. K. Relationships between specific ultraviolet absorbance and trihalomethane precursors of different carbon sources. *J. Water Supply Res. Tehnol.* **2008**, *57*, 471−480.

(4) Grayson, R.; Holden, J. Continuous measurement of spectrophotometric absorbance in peatland streamwater in northern England: implications for understanding fluvial carbon fluxes. *Hydrol. Process.* **2012**, *26*, 27−39.

(5) Porcal, P.; Koprivnjak, J.-F.; Molot, L. A.; Dillon, P. J. Humic substances − part 7: the biogeochemistry of dissolved organic carbon and its interactions with climate change. *Environ. Sci. Pollut. Res.* **2009**, *16*, 714−726.

(6) Bernhardt, E. S.; Likens, G. E. Dissolved organic carbon enrichment alters nitrogen dynamics in a forest stream. *Ecology* **2002**, *83*, 1689−1700.

(7) Worrall, F.; Parker, A.; Rae, J. E.; Johnson, A. C. A study of the sorption kinetics of isoproturon on soil and subsoil: The role of dissolved organic carbon. *Chemosphere* **1997**, *34*, 87−97.

(8) Tsui, M. T. K.; Finlay, J. C. Influence of dissolved organic carbon on methylmercury bioavailability across Minnesota stream ecosystems. *Environ. Sci. Technol.* **2011**, *45*, 5981−5987.

(9) Jollymore, A.; Johnson, M. S.; Hawthorne, I. Submersible UV−vis spectroscopy for quantifying streamwater organic carbon dynamics: implementation and challenges before and after forest harvest in a headwater stream. *Sensors* **2012**, *12*, 3798−3813.

(10) Strohmeier, S.; Knorr, K.-H.; Reichert, M.; Frei, S.; Fleckenstein, J. H.; Peiffer, S.; Matzner, E. Concentrations and fluxes of dissolved organic carbon in runoff from a forested catchment: insights from high frequency measurements. *Biogeosciences* **2013**, *10*, 905−916.

(11) Inamdar, S. P.; Singh, S.; Dutta, S.; Levia, D.; Mitchell, M.; Scott, D.; Bais, H.; McHale, P. Fluorescence characteristics and sources of dissolved organic matter for stream water during storm events in a forested mid-Atlantic watershed. *J. Geophys. Res.* **2011**, *116*, 10.1029/2011JG001735.

(12) Marks, R. J. *Introduction to Shannon Sampling and Interpolation Theory*; Springer-Verlag: New York, 1991.

(13) Littlewood, I. G.; Croke, B. F. W. Effects of data time-step on the accuracy of calibrated rainfall−streamflow model parameters: practical aspects of uncertainty reduction. *Hydrol. Res.* **2013**, *44*, 430−440.

(14) Young, P. C. The estimation of continuous-time rainfall-flow models for flood risk management. In *Role of Hydrology in Managing Consequences of a Changing Global Environment*; Walsh, C., Ed.; British Hydrological Society: Newcastle upon Tyne, 2010; pp 303−310.

(15) Box, G. E. P., Jenkins, G. M., Reinsel, G. C. *Time Series Analysis: Forecasting and Control*, 4th ed.; Wiley: Hoboken, 2008.

(16) Jones, T. D.; Chappell, N. A. Streamflow and hydrogen ion interrelationships identified using Data-Based Mechanistic modelling of high frequency observations through contiguous storms. *Hydrol. Res.* **2014**, 10.2166/nh.2014.155.

(17) Moldan, F.; Hruska, J.; Evans, C. D.; Hauhs, M. Experimental simulation of the effects of extreme climatic events on major ions, acidity and dissolved organic carbon leaching from a forested catchment, Gardsjon, Sweden. *Biogeochemistry* **2012**, *107*, 455−469.

(18) Jeong, J.-J.; Bartsch, S.; Fleckenstein, J.; Matzner, E.; Tenhunen, J. D.; Lee, S. D.; Park, S. D.; Park, J.-H. Differential storm responses of dissolved and particulate organic carbon in a mountainous headstream, investigated by high-frequency in-situ optical measurements. *J. Geophys. Res.* **2012**, *117*, G03013.

(19) Waterloo, M. J.; Oliveira, S. M.; Drucker, D. P.; Nobre, A. D.; Cuartas, L. A.; Hodnett, M. G.; Langedijk, I.; Jans, W. W. P.; Tomasella, J.; de Araújo, A. C.; Pimentel, T. P.; Múnera, J. C. Export of organic carbon in run-off from an Amazonian rainforest blackwater catchment. *Hydrol. Process.* **2006**, *20*, 2581−2597.

(20) Koehler, A. K.; Murphy, K.; Kiely, G.; Sottocornola, M. Seasonal variation of DOC concentration and annual loss of DOC from an Atlantic bog in South Western Ireland. *Biogeochemistry* **2009**, *95*, 231−242.

(21) Parker, G. T.; Droste, R. L.; Rennie, C. D. Coupling model uncertainty for coupled rainfall/runoff and surface water quality models in river problems. *Ecohydrology* **2013**, *6*, 845−851.

(22) Hornberger, G. M.; Bencala, K. E.; McKnight, D. M. Hydrological controls on dissolved organic carbon during snowmelt in the Snake River near Montezuma, Colorado. *Biogeochemistry* **1994**, *25*, 147−165.

(23) Taugbøl, G.; Seip, H. M.; Bishop, K.; Grip, H. Hydrochemical modelling of a stream dominated by organic acids and organically bound aluminium. *Water, Air, Soil Pollut.* **1993**, *78*, 103−139.

(24) Boyer, E. W.; Hornberger, G. M.; Bencala, K. E.; McKnight, D. Overview of a simple model describing variation of dissolved organic carbon in an upland catchment. *Ecol. Modell.* **1996**, *86*, 183−188.

(25) Boyer, E. W.; Hornberger, G. M.; Bencala, K. E.; McKnight, D. M. Effects of asynchronous snowmelt on flushing of dissolved organic carbon: a mixing model approach. *Hydrol. Process.* **2000**, *14*, 3291−3308.

(26) Futter, M. N.; Butterfield, D.; Cosby, B. J.; Dillon, P. J.; Wade, A. J.; Whitehead, P. G. Modeling the mechanisms that control in-stream dissolved organic carbon dynamics in upland and forested catchments. *Water Resour. Res.* **2007**, *43*, W02424.

(27) Futter, M. N.; Löfgren, S.; Köhler, S. J.; Lundin, L.; Moldan, F.; Bringmark, L. Simulating dissolved organic carbon dynamics at the

Swedish Integrated Monitoring Sites with the Integrated Catchments Model for Carbon, INCA-C. *Ambio* **2011**, *40*, 906−919.
(28) Ågren, A.; Haei, M.; Köhler, S.; Bishop, K.; Laudon, H. Regulation of stream water dissolved organic carbon (DOC) concentrations during snowmelt; the role of discharge, winter climate and memory effects. *Biogeosciences* **2010**, *7*, 2901−2913.
(29) Grieve, I. C. A model of dissolved organic carbon concentrations in soil and stream waters. *Hydrol. Process.* **1991**, *5*, 301−307.
(30) Liu, W.; Xu, X.; McGoff, N. M.; Eaton, J. M.; Leahy, P.; Foley, N.; Kiely, G. Spatial and seasonal variation of dissolved organic carbon (DOC) concentrations in Irish streams: importance of soil and topography characteristics. *Environ. Manage.* **2014**, *53*, 959−67.
(31) Rier, S. T.; Stevenson, R. J.; LaLiberté, G. D. Photo-acclimation response of benthic stream algae across experimentally manipulated light gradients: a comparison of growth rates and net primary productivity. *J. Phycol.* **2006**, *42*, 560−567.
(32) Rowland, A. P.; Neal, C.; Reynolds, B.; Neal, M.; Lawlor, A. J.; Sleep, D. Manganese in the upper Severn mid-Wales. *J. Environ. Monit.* **2012**, *14*, 155−164.
(33) Box, G. E. P.; Jenkins, G. M. *Time Series Analysis: Forecasting and Control*, 1st ed.; Holden-Day: San Francisco, 1970.
(34) Young, P. C. The refined instrumental variable method. *J. Eur. Syst. Autom.* **2008**, *42*, 149−179.
(35) Taylor, C. J.; Pedregal, D. J.; Young, P. C.; Tych, W. Environmental time series analysis and forecasting with the Captain Toolbox. *Environ. Modell. Software* **2007**, *22*, 797−814.
(36) Jakeman, A. J.; Littlewood, I. G.; Whitehead, P. G. An assessment of the dynamic response characteristics of streamflow in the Balquhidder catchments. *J. Hydrol.* **1993**, *145*, 337−355.
(37) Freeman, C.; Evans, C. D.; Monteith, D. T. Export of organic carbon from peat soils. *Nature* **2001**, *412*, 785.
(38) Clark, J. M.; Chapman, P. J.; Adamson, J. K.; Lane, S. N. Influence of drought-induced acidification on the mobility of dissolved organic carbon in peat soils. *Global Change Biol.* **2005**, *11*, 791−809.
(39) Beven, K.; Young, P. A guide to good practice in modeling semantics for authors and referees. *Water Resour. Res.* **2013**, *49*, 5092−5098.
(40) Grieve, I. C. Seasonal, hydrological, and land management factors controlling dissolves organic carbon concentrations in the loch fleet catchments, Southwest Scotland. *Hydrol. Process.* **1990**, *4*, 231−239.
(41) Hinton, M. J.; Schiff, S. L.; English, M. C. The significance of runoff events on the concentrations and export of dissolved organic carbon from two Precambrian Shield watersheds. *Biogeochemistry* **1997**, *36*, 67−88.
(42) Dawson, J. J. C.; Billett, M. F.; Neal, C.; Hill, S. A comparison of particulate, dissolved and gaseous carbon in two contrasting upland streams in the UK. *J. Hydrol.* **2002**, *257*, 226−246.
(43) McDowell, W. H.; Likens, G. E. Origin, composition, and flux of dissolved organic carbon in the Hubbard Brook Valley. *Ecol. Monogr.* **1998**, *58*, 177−195.
(44) Bestland, E.; Milgate, S.; Chittleborough, D.; VanLeeuwen, J.; Pichler, M.; Soloninka, L. The significance and lag-time of deep through flow: an example from a small, ephemeral catchment with contrasting soil types in the Adelaide Hills, South Australia. *Hydrol. Earth Syst. Sci.* **2009**, *13*, 1201−1214.
(45) Young, P. C. Recursive estimation, forecasting and adaptive control. In *Control and Dynamic Systems: Advances in Theory and Applications*; Leondes, C. T., Ed.; Academic Press: San Diego, 1990; pp 119−166.
(46) Ockenden, M. C.; Chappell, N. A. Identification of the dominant runoff pathways from the data-based mechanistic modelling of nested catchments in temperate UK. *J. Hydrol.* **2011**, *402*, 71−79.
(47) Chappell, N. A.; Ternan, J. L.; Williams, A. G.; Reynolds, B. Preliminary analysis of water and solute movement beneath a coniferous hillslope in mid-Wales, UK. *J. Hydrol.* **1990**, *116*, 201−215.
(48) Soulsby, C.; Reynolds, B. Modelling hydrological processes and aluminium leaching in an acid soil at Llyn Brianne, Mid-Wales. *J. Hydrol.* **1992**, *138*, 409−429.
(49) Worrall, F.; Burt, T. P.; Jaeban, R. Y.; Warburton, J.; Shedden, R. Release of dissolved organic carbon from upland peat. *Hydrol. Process.* **2002**, *16*, 3487−3504.
(50) Hood, E.; Gooseff, M. N.; Johnson, S. L. Changes in the character of stream water dissolved organic carbon during flushing in three small watersheds, Oregon. *J. Geophys. Res.* **2006**, *111*, G01007.
(51) Morel, B.; Durand, P.; Jaffrezic, A.; Gruau, G.; Molenat, J. Sources of dissolved organic carbon during stormflow in a headwater agricultural catchment. *Hydrol. Process.* **2009**, *23*, 2888−2901.
(52) Shipitalo, M. J.; Edwards, W. M. Effects of initial water content on macropore/matrix flow and transport of surface-applied chemicals. *J. Environ. Qual.* **1996**, *25*, 662−670.
(53) Inamdar, S. P.; O'Leary, N.; Mitchell, M. J.; Riley, J. T. The impact of storm events on solute exports from a glaciated forested watershed in western New York. *Hydrol. Process.* **2006**, *20*, 3423−3439.
(54) Hruska, J.; Kram, P.; McDowell, W. H.; Oulehle, F. Increased dissolved organic carbon (DOC) in Central European streams is driven by reductions in ionic strength rather than climate change or decreasing acidity. *Environ. Sci. Technol.* **2009**, *43*, 4320−4326.
(55) Spencer, R. G. M.; Hernes, P. J.; Aufdenkampe, A. K.; Baker, A.; Gulliver, P.; Stubbins, A.; Aiken, G. R.; Dyda, R. Y.; Butler, K. D.; Mwamba, V. L.; Mangangu, A. M.; Wabakanghanzi, J. N.; Six, J. An initial investigation into the organic matter biogeochemistry of the Congo River. *Geochim. Cosmochim. Acta* **2012**, *84*, 614−627.
(56) Allpike, B. P.; Heitz, A.; Joll, C. A.; Kagi, R. I.; Abbt-braun, G.; Frimmel, F. H.; Brinkmann, T.; Her, N.; Amy, G. Size exclusion chromatography to characterize DOC removal in drinking water treatment. *Environ. Sci. Technol.* **2005**, *37*, 2334−2342.